IEEE Access
Multidisciplinary | Rapid Review | Open Access Journal

Received 30 October 2023, accepted 1 December 2023, date of publication 12 December 2023,
date of current version 19 December 2023.

Digital Object Identifier 10.1109/ACCESS.2023.3341884

RESEARCH ARTICLE

Design and Implementation of Optimal Control Scheme for DFIG Based Wind Plant to Mitigate Sub-Synchronous Resonance Issues

SAIF UL ISLAM AND SOOBAE KIM
Department of Electrical Engineering, School of Electronic and Electrical Engineering, Kyungpook National University, Daegu 41566, South Korea
Corresponding author: Soobae Kim (soobae.kim@knu.ac.kr)

This work was supported by the BK21 Four Project funded by the Ministry of Education, Republic of Korea, under Grant 4199990113966.

ABSTRACT This article presents an investigation of sub-synchronous resonance (SSR) issues in doubly-fed induction generator (DFIG) based wind plant and proposes an optimal control scheme for its mitigation. The article firstly reviews the causes of SSR, namely compensation level and wind speed in DFIG-based wind plant. The proportional resonance controller with harmonic compensators (PR+HC) is designed to mitigate SSR without compromising total harmonic distortions (THD) in the power signal. The series compensated IEEE first benchmarked model energized with a 100MW DFIG-based wind plant is used as a platform in MATLAB/Simulink for the implementation of the proposed scheme. The comparative analysis of the designed PR+HC controller is carried out with the conventional Proportional Integral (PI) controller to validate the optimal response of PR+HC controller. In addition, high performance of PR+HC in coordination with a flexible AC transmission (FACT) device in terms of damped oscillations and low THD is achieved. The overall simulation results are analyzed in both time domain and frequency domain to authenticate the damped, low harmonic, and smooth response of proposed scheme under varying compensation level and wind speeds.

INDEX TERMS Renewable energy resources, DFIG-based wind plant, flexible AC transmission devices, harmonic compensators, optimization, proportional resonant controller, sub-synchronous resonance.

I. INTRODUCTION

The boost in affinity for utility scale renewable energy resources (RERs) has been observed in the advanced world due to the rapid exhaustion of fossil energies and a shift in energy policy towards carbon free electric resources [1], [2]. Currently, wind energy resources are leading the electric power market among the existing RERs [3], [4], [5]. Utility scale wind energy plants are installed at the windy areas regardless of consumers load points, and the energy can be delivered to the load centers through a transmission network. As the load demand increases, more wind plants has to be installed, requiring an expansion of the transmission network by laying extra lines.

The associate editor coordinating the review of this manuscript and approving it for publication was Arturo Conde.

However, installation of a new transmission line for marginally extra load demand is not cost-effective and obtaining the right of way (ROW) for new lines is usually not permissible in highly populated areas. Alternatively, the power transfer capacity of the existing network is augmented through fixed series compensation (FSC), which can also increase the margin of transient stability [6], [7]. Despite the financial benefits with FSC, it can be prone to the consequences of sub-synchronous resonance (SSR) due to the direct interaction of FSC transmission lines and generating plants [8].

The extensive integration of wind plant resources to the grid has modified the existing power system characteristics and made it more complex [9]. The phenomenon of SSR in doubly fed induction generator (DFIG)-based wind plants gained significant consideration when it occurred in the

southern utility grid in Texas in 2009 [10]. Similarly, SSR oscillations were also identified in Minnesota, and the most recent SSR case in DFIG-based wind plant was observed in Hebei province, China, in 2012 [11], [12]. The investigation analysis reveals that such sub-synchronous oscillations (SSO) are similar to the induction-generator effect (IGE), which is actuated by exceeding the rotor negative resistance from the overall network resistance at a frequency lower than rated system frequency, i.e., sub-synchronous frequency [13]. Such an IGE can occur in wind plant-based DFIG integrated with an FSC transmission line, depending upon the level of series compensation and wind speed [14].

To counteract such events, various strategies has been presented to mitigate the oscillations due to SSR in GFIGs. These strategies can be classified into two types: flexible AC transmission systems (FACTS)-based and control-based. The FACTS-based strategies use electronic-based switched devices such as thyristor-controlled series capacitor (TCSC), static synchronous compensator (STATCOM), and gate-controlled series capacitor (GCSC), etc., [15], [16], [17]. These devices can mitigate SSR oscillations in DFIG-based wind plants significantly but compromise on the harmonic distortions in the power signal due to their electronic switching and are costly [18]. Alternatively, the control-based strategies are cost-effective but result in low-damped and late-settling response of electrical variables compared to FACTS strategies. Control-based strategies at both rotor-side converter (RSC) and grid-side converter (GSC) of DFIG have been extensively studied in the literature. The conventionally used proportional-integral (PI) controller is adopted by the IEEE first benchmarked model integrated with DFIG-based wind plants due to its simplicity and easy implementation. An additional linear controller is employed at the GSC to restrict the SSR oscillation; however, its optimal response is constrained to the power rating of GSC [19]. To overcome the issue of GSC capacity, an additional controller is proposed at RSC; in other words, the linear converter gain is divided into both sides of the back-to-back converter [20]. However, this design requires measurement of the voltage of the series compensator and is prone to sub-synchronous control interaction (SSCI). Taking advantage of multi-input-multi-output (MIMO), the authors in [21] presented a control scheme on the basis of optimal state feedback. In [22], a control scheme for SSR damping is proposed through phase compensation using lead-lag filters. This technique is simple to design and tune compared to the previously mentioned model-based schemes.

The methodologies mentioned above are related to the linearized interpretation of the system, although the series compensated transmission system integrated with wind plant is non-linear in nature. So, the performance of the linear controller can be affected during operations beyond the linearized limit where the controller is designed. To handle this limitation, partial feedback linearization (PFL) and high switching frequency controller, i.e., sliding mode control (SMC) schemes, are implemented for SSR dampening in

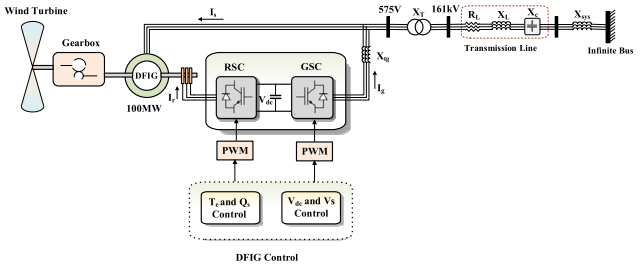

FIGURE 1. Adopted IEEE first benchmark model of a DFIG-based wind plant.

DFIG-based wind plants. These nonlinear controllers can ensure effective SSR oscillation mitigation in nonlinear systems; however, the design process requires multiple stages and lacks arrangement for harmonic elimination.

The key contributions of this article are listed below:

1. An optimal control scheme, i.e., proportional resonance controller in coordination with harmonic compensators (PR+HC), is designed to mitigate SSR in DFIG-based wind plants without compromising total harmonic distortions (THD).
2. The modified series fixed compensated IEEE first benchmark model (IBM) integrated with DFIG-base wind plant is adopted as a test environment for the implementation of the proposed optimal control scheme.
3. Simulation responses are analyzed in time domain and frequency domain to authenticate the effective SSR mitigating nature of the proposed scheme at various compensation levels and wind speeds.
4. The THD reduction capability of the proposed control scheme is investigated in one of the popular FACTS devices, i.e., TCSC through fast Fourier transformation (FFT) tool in MATLAB/Simulink.
5. The overall results of the above-mentioned analytical approaches are compared with the conventionally used well-tuned PI controller, individually and in combination with TCSC, for the justification of the better performance of the designed scheme.

The remaining paper is categorized as follows: system modeling in Section II, control structure in Section III, results and discussions in Section IV, and conclusion Section V.

II. SYSTEM MODELING

The IEEE first benchmark platform has been modified by replacing the synchronous rotating machine with the DFIG-based wind plant to analyze the SSR behavior in DFIG, as depicted in Fig.1 [25], [26]. A 100 MW aggregated wind model consisting of 67 turbines, each with a capacity of 1.5 MW, is employed for the study. The 575 V output voltage of the DFIG is coupled with a 161 kV FSC transmission line via step-up transformer for integration with a strong grid.

The detailed system parameters are given in Table 1 of appendix. The state-space representation of fundamental

components for the test platform is required to analyze the SSR effect as below.

A. WIND TURBINE MODEL

The mechanical output torque of wind turbine (T_{mech}) is directly dependent on the square of the wind speed (W_V) as in (1) as in [28].

$$T_{mech} = \frac{\rho R_r A C_p W_V^2}{2\lambda} \tag{1}$$

The remaining dependent parameters ρ, R_r, A, λ represents the air density, the turbine's rotor radius, the sweep area of the blade, and the tip speed ratio, respectively. However, the power constant of the blade C_P, which depends upon the pitch angle of the blade "θ_p" and the tip speed ratio as follow.

$$C_P = 0.5\left(\frac{RD_c}{\lambda} - 0.022 * \theta_p - 2.0\right) e^{-0.255\left(\frac{RD_c}{\lambda}\right)} \tag{2}$$

Here "D_c'' is the design coefficient of the blade and the tip speed ratio "λ'' can be calculated as in (3).

$$\lambda = \frac{\Omega_{mech}.r_R}{W_V} \tag{3}$$

where Ω_{mech} and r_R are the mechanical angular velocity and the rotor radius of turbine, respectively.

B. SHAFT MODELING

The shaft of a DFIG based wind plant is characterized by the two-mass tortional dynamics. The wind turbine side shaft is represented as a low-speed, while the DFIG side shaft is represented as a high-speed second mass. This two-mass shaft is represented in state-space as below [28]:

$$\frac{d}{dt}\begin{pmatrix}\omega_t\\ \omega_r\\ T_g\end{pmatrix} = \begin{pmatrix}\frac{-D_t-D_g}{2H_t} & \frac{D_g}{2H_t} & \frac{-1}{2H_t}\\ \frac{D_g}{2H_g} & \frac{-D_g-D_t}{2H_g} & \frac{-1}{2H_g}\\ K_{tg}\omega_g & K_{tg}\omega_e & 0\end{pmatrix}\begin{pmatrix}\omega_t\\ \omega_r\\ T_g\end{pmatrix} + \begin{pmatrix}\frac{T_{em}}{2H_t}\\ \frac{-T_{ele}}{2H_t}\\ 0\end{pmatrix} \tag{4}$$

Here, T_{em} and T_{ele} are the input parameters of the shaft model and ω_t, ω_r, T_g are state-space variables, which represent the speed of the wind turbine, the speed of the rotor and the internal torque of the system, respectively. D_t, H_t, and D_g, H_g are the damping and inertia constants of the wind turbine and generator, respectively. K_{tg} represents the shaft stiffness between the two coupled masses.

Moreover, due the coupling of wind turbine shaft and generator rotor through a gearbox, the whole turbine cannot be considered as a stiff. To accurately address this influence, an extra equation has been incorporated to characterize the twist of the whole shaft [27].

$$2H_t\frac{d\Omega_{mech}}{dt} = T_m - T_w \tag{5}$$

Here T_w is the prime torque on the shaft by wind and T_m is the mechanical torque acts on the rotor of generator. Further T_m can be characterized as a twisting angle between the prime wind turbine shaft and generator rotor as (6).

$$T_m = K_{stif}(\theta_r - \theta_m) \tag{6}$$

Here, θ_r and θ_m are the positions of generator rotor angle and wind turbine shaft, whereas K_{stif} is the stiffness coefficient.

C. DFIG MODELING

The dynamical model of order six is represented as [29].

$$\dot{X} = A_D X_D + B_D U_D \tag{7}$$

Here X_D and U_D represent the state input variables i.e., currents and voltages of DFIG as:

$$X_D = [i_{ds}; i_{qs}; i_{0s}; i_{dr}; i_{qr}; i_{or}] \tag{8}$$

$$X_D = [v_{ds}; v_{qs}; v_{0s}; v_{dr}; v_{qr}; v_{or}] \tag{9}$$

The variables in (8), i_{ds}, i_{qs} and i_{dr}, i_{qr} denote the active and reactive components of the stator and rotor currents, respectively. Similarly, v_{ds}, v_{qs} and v_{dr}, v_{qr} in (9) denote the active and reactive voltage components of the stator and rotor, respectively. while i_{0s}, i_{0r} and v_{0s}, v_{0r} are the zero sequence currents and voltages are zero due to the balance system.

The constants of state variables A_D and B_D can be represented as (10) and (11), as shown at the bottom of the next page.

In the above (10) and (11), the parameters R_S and R_r denote the resistance, while X_S and X_r denote the reactance of the stator and rotor, respectively. However, X_{lS} and X_{lr} are the leakage reactance of the stator and rotor. Further, X_M is the mutual reactance between the stator and rotor.

D. DC-LINK MODELING

The dynamical response of the dc-link capacitor (C_{dc}) used for coupling GSC and RSC can be represented by s first-order dynamic model as [29].

$$C_{dc}V_{dc}\frac{dV_{dc}}{dt} = P_R - P_G \tag{12}$$

Whereas P_R and P_G are the rotor side and grid side powers and can be calculated as:

$$P_R = \frac{1}{2}(v_{dr}i_{dr} + v_{qr}i_{qr}) \tag{13}$$

$$P_G = \frac{1}{2}\left(v_{dg}i_{qg} + v_{qg}i_{qg}\right) \tag{14}$$

Here, v_{dr}, v_{qr} and i_{dr},i_{qr} are the active and reactive parts of the rotor side voltage and current. While v_{dg}, v_{qg} and i_{dg},i_{qg} represent the active and reactive parts of the grid side voltage and current, respectively.

E. MODELING OF FSC TRANSMISSION LINE

In general, the dynamical modeling of the FSC model is the main area for SSR analysis [29]. The transmission line is assumed electrically as a lumped RLC circuit and can be implemented in the synchronous reference frame to model

the FSC line. The dynamic equations for each phase are given as [25]:

$$R_l.i_l + L\frac{di_l}{dt} + v_{FSC} = v_s - V_B \tag{15}$$

$$C\frac{dv_{FSC}}{dt} = i_l \tag{16}$$

The state-space characterization of the FSC transmission line can be written as:

$$\frac{d}{dt}\begin{pmatrix} i_{ql} \\ i_{dl} \\ v_{FSCq} \\ v_{FSCd} \end{pmatrix} = \begin{pmatrix} -\frac{R_l}{X_l} & -\omega_e & -\frac{1}{X_l} & 0 \\ -\omega_e & -\frac{R_l}{X_l} & 0 & -\frac{1}{X_l} \\ X_{FSC} & 0 & 0 & -\omega_e \\ 0 & X_{FSC} & \omega_e & 0 \end{pmatrix} \begin{pmatrix} i_{ql} \\ i_{dl} \\ v_{FSCq} \\ v_{FSCd} \end{pmatrix} + \omega_b \begin{pmatrix} \frac{v_{qs}-V_{Bq}}{X_l} \\ \frac{v_{ds}-V_{Bd}}{R_l} \\ 0 \\ 0 \end{pmatrix} \tag{17}$$

In the above (13)-(15), v_s, V_B and v_{FSC} denotes source bus, infinite bus and FSC voltages respectively, whereas R_l, X_l and i_l denotes line resistance, reactance and current. However, the remaining parameters with subscript d and q represents the active and reactive parts of the mentioned parameters, while ω_e, ω_b are synchronous reference and base speeds respectively.

III. CONTROL STRUCTURE

The control structure of the proposed DFIG-based wind platform is comprised of back-to-back converters, i.e., rotor side and grid side, as in Figure 1.The pulse width modulation (PWM) signals for these converters are maintained via a PI controller conventionally. The purpose of the traditionally used PI controller implemented in the benchmark series compensated DFIG model is error compensation through proportional and integral gains during steady state. However, the PI controller has some constraints of sensitivity for parametric variables and dynamic conditions, like during large disturbances, the PI controller loses its anti-windup capability. Additionally, until now, the presented controller for DFIG converters must be designed for both GSC and RSC, which needs a lot of computations. Alternatively, this paper presents a hybrid control scheme, i.e., PR with HC scheme, which can provide damping to the frequencies other than the system synchronous frequency only by optimal control of dc-link voltage, i.e., Vdc at GSC.

A. DESIGN OF THE PROPOSED CONTROLLER (PR+HC)

The proposed control scheme is the coordination of two parts, i.e., PR controller and harmonic compensators, as shown in Fig.2. The fundamental PR controller is used for compensation of error between measured and reference signal, much similar to the PI controller, but the PR controller maintains the synchronism due to its integration capability near the resonance frequency. The second part is harmonic compensators (HC) operating simultaneously with the main PR controller to suppress the harmonic components in the signal to enhance the power quality. The proposed scheme is the digital implementation of s parallel-resonant fault current limiter (PRFCL), which is a FACTS-based fault current limiter that provides high impedance without phase shift for fault current.

The proposed scheme provides high impedance gain at the resonant frequency and low gain at other frequencies. So, it can mitigate the SSR oscillation due to resonance between line inductance and FSC matching without any steady-state error in the power signal. The control scheme is implemented for dc-link voltage regulation because it is the common link between RSC and GSC. The fundamental part of the proposed controller, i.e., PR controller, is comprised of two terms again as the proportional term and resonant term expressed below in (18) [30].

$$G_{PR}(s) = K_P + \frac{2K_i\omega_c s}{s^2 + 2\omega_c s + (\omega_0)^2} \tag{18}$$

Here, K_P, K_i and ω_0 are the proportional gain, integral gain, and resonant frequency, respectively. The cutoff frequency ω_c is used in the transfer function to avoid instability by limiting the ideal PR controller to a finite gain. The cutoff frequency can be selected much lower than the resonant frequency i.e., 1.6% of the resonant frequency [30].

$$A_D = -B_D \begin{pmatrix} R_S & \frac{\omega_S}{\omega_b}X_S & 0 & 0 & \frac{\omega_S}{\omega_b}X_M & 0 \\ -\frac{\omega_S}{\omega_b}X_S & R_S & 0 & -\frac{\omega_S}{\omega_b}X_M & 0 & 0 \\ 0 & 0 & R_S & 0 & 0 & 0 \\ 0 & \frac{\omega_S-\omega_r}{\omega_b}X_M & 0 & R_r & \frac{\omega_S-\omega_r}{\omega_b}X_r & 0 \\ -\frac{\omega_S-\omega_r}{\omega_b}X_M & 0 & 0 & -\frac{\omega_S-\omega_r}{\omega_b}X_r & R_r & 0 \\ 0 & 0 & 0 & 0 & 0 & R_r \end{pmatrix} \tag{10}$$

$$B_D = -\omega_b \begin{pmatrix} X_S & 0 & 0 & X_M & 0 & 0 \\ 0 & X_S & 0 & 0 & X_M & 0 \\ 0 & 0 & X_{lS} & 0 & 0 & 0 \\ X_M & 0 & 0 & X_r & 0 & 0 \\ 0 & X_M & 0 & 0 & X_r & 0 \\ 0 & 0 & 0 & 0 & 0 & X_{lr} \end{pmatrix}^{-1} \tag{11}$$

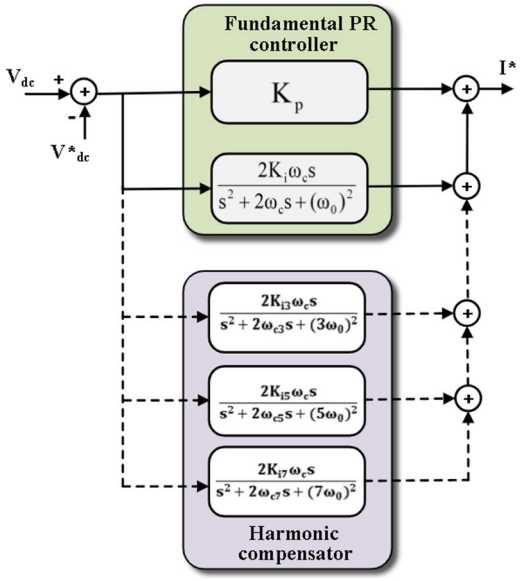

FIGURE 2. Design of PR controller with HC.

An additional part of the proposed controller is harmonic compensators (HC), which is employed to minimize the distortions in the power signal resulted by switching devices. The non-ideal finite transfer function $G_{HC}(s)$ for damping the harmonic components is given by (19) as follows.

$$G_{HC}(s) = \sum_{h=3,5,7} G_{HCh}(s) \tag{19}$$

whereas,

$$G_{HCh}(s) = \frac{2K_{ih}\omega_{ch}s}{s^2 + 2\omega_{ch}s + (h\omega_0)^2} \tag{20}$$

The above harmonic compensators operate in parallel with the fundamental PR controller to dampen the 3rd, 5th, and 7th harmonic frequencies. The damping factor (σ) and cutoff frequencies for corresponding harmonic components (ω_{ch}) can be achieved using (21) and (22) as in [31] and [32].

$$\sigma = \frac{\omega_{ch}}{h.\omega_0} \tag{21}$$

$$\omega_{ch} = \sum_{h=3,5,7} (h.\omega_c) \tag{22}$$

The overall parameters for the designed control scheme are listed in Table 2 of appendix.

IV. RESULTS AND DISCUSSION

The output response of the proposed control scheme is analyzed by varying compensation level and wind speed at the IEEE first benchmark series compensated DFIG-based wind plant. To verify the SSR mitigation capability of the proposed controller, the MATLAB simulation results are carried out in both time domain and frequency domain. Further, the comparative analysis is carried out with the conventionally adopted PI controller to justify the damped oscillations without actuating SSR at other frequencies. Additionally, harmonic distortions in the power signal with PR+HC controller and PI controller are calculated and compared by hybrid operation of FACTS device, i.e., TCSC. The detailed simulation results with three different techniques are presented below to authenticate the harmonic-free damped SSR oscillation.

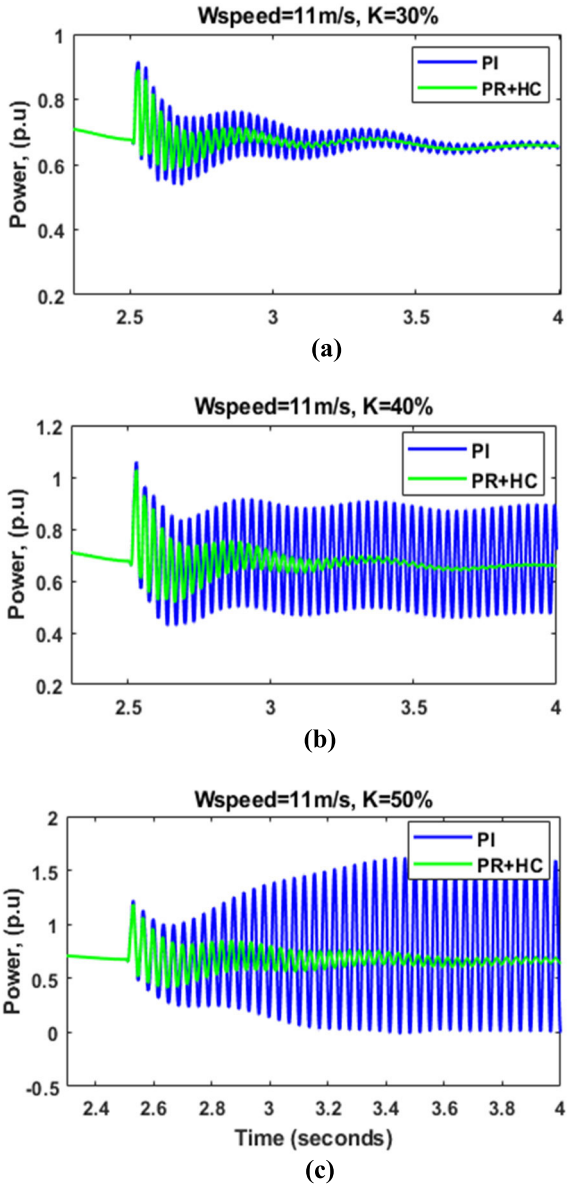

FIGURE 3. Response of sub-synchronous oscillations in the time domain (a, b, c) at different compensation levels.

A. TIME DOMAIN AND FREQUENCY DOMAIN RESPONSES

The behavior of the proposed scheme through time domain simulations and frequency scanning is discussed at different compensation levels and wind speeds.

1) IMPACT OF COMPENSATION LEVEL

The network impedance characteristics of the adopted IEEE first benchmark DFIG-based wind plant are changed through

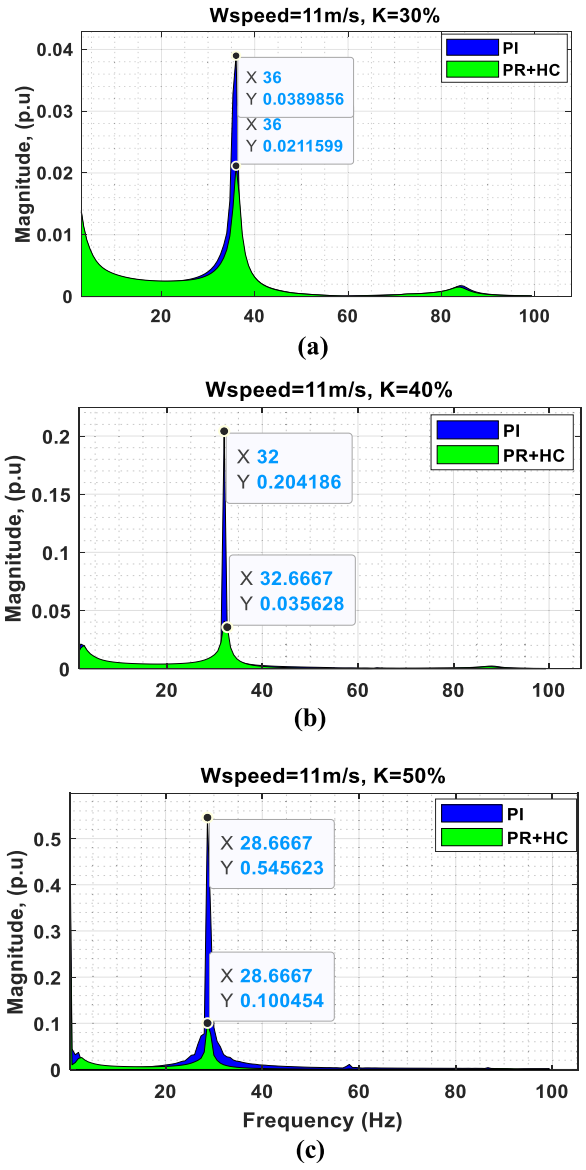

FIGURE 4. Response of sub-synchronous oscillations in frequency domain (a, b, c) at different compensation levels.

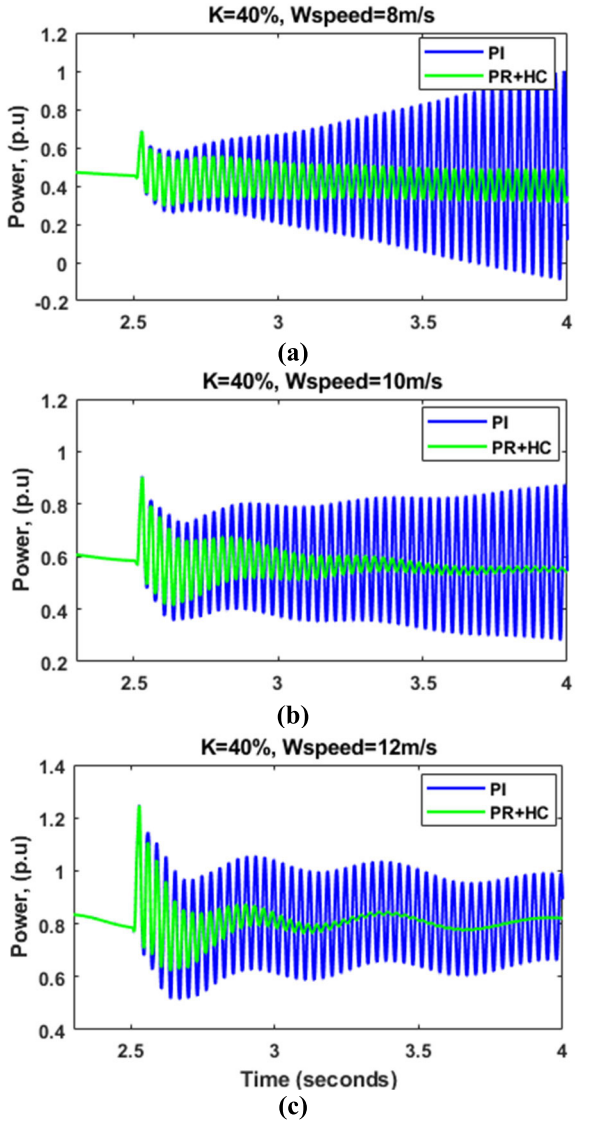

FIGURE 5. Response of sub-synchronous oscillations in the time domain (a, b, c) at different wind speeds.

different compensation levels in percentage to the rated impedance of the line. The FSC of various levels, i.e., 30%, 40% and 50%, is inserted at time 2.5 sec while keeping the wind speed constant, i.e., 11m/s to analyze the impact of compensation level. As the level of series compensation increases, the system is becoming more prone to SSR oscillations in the power signal as depicted by figure 3 and figure 4. At some specific level of compensation where the effective internal impedance of the DFIG becomes negative, the sub-synchronous oscillations grow with time and the system becomes unstable [14]. The proposed controller is tuned in such a way that it provides high impedance gain to the SSR at a particular sub-synchronous frequency. The time domain responses in Figure 3 (a, b, c) clearly show that the severity of SSR is directly proportional to the compensation level. The response with conventional PI controller gives critically damped oscillation at 40% compensation as in Figure 3(b), and even becomes unstable at 50% of compensation level as depicted by Figure 3(c). However, in the case of the proposed PR+HC controller, although there is an increase in oscillations with the level of compensation, it has a significantly low magnitude and stable response comparatively as presented in Figure 3(a, b, c).

To justify the optimal response of the proposed scheme, frequency domain analysis reflects the same efficient response as in time domain analysis at various compensation levels. Figure 4(a, b, c) shows that the increase in compensation level results in increasing magnitude of power oscillation in per unit (p.u) and decreasing in sub-synchronous frequency. However, in the frequency scanning analysis the proposed scheme gives significantly minimum

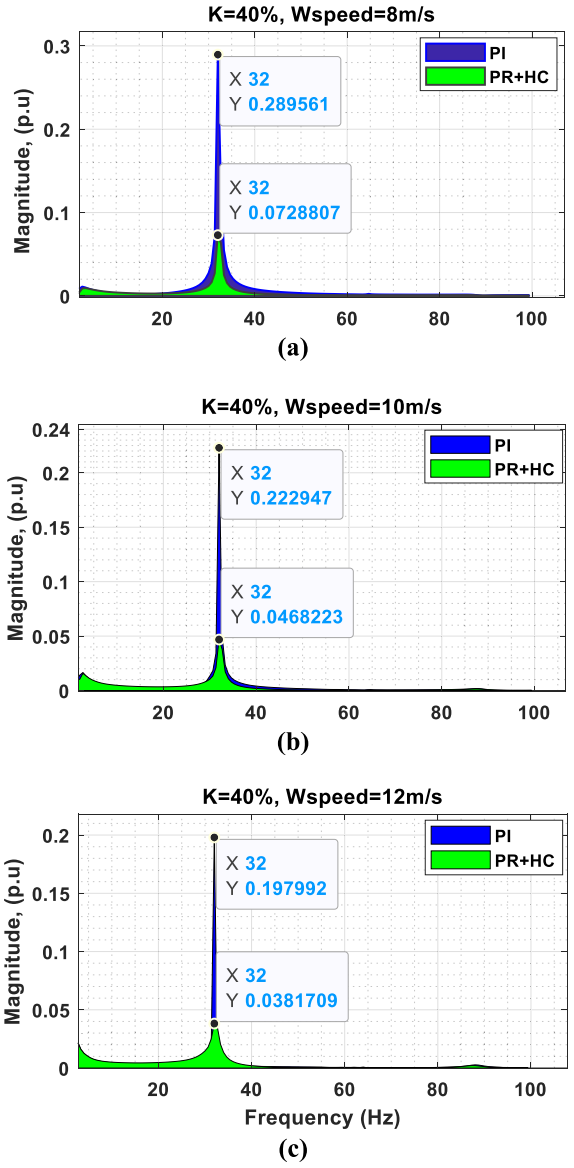

FIGURE 6. Response of sub-synchronous oscillations in the frequency domain (a, b, c) at different wind speeds.

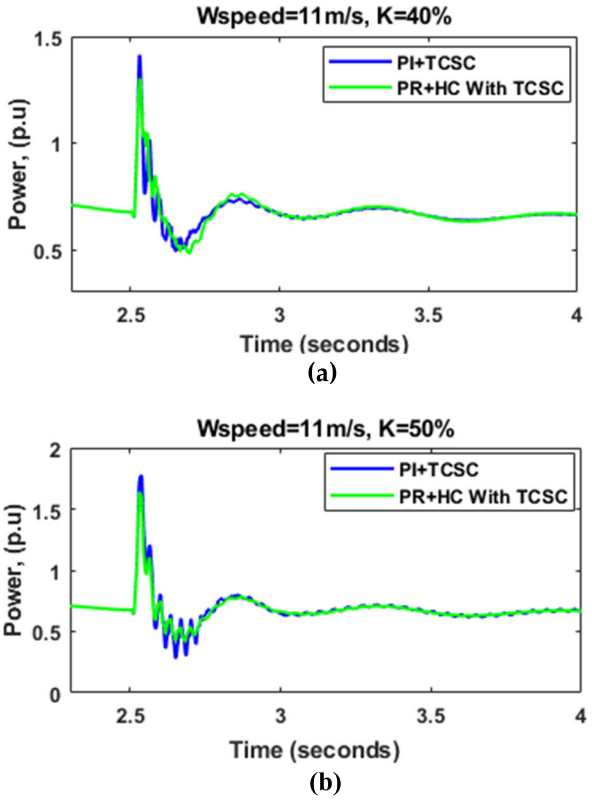

FIGURE 7. Response of sub-synchronous oscillations in the time domain (a, b) at different compensation levels by including TCSC.

magnitude of SSO as compared to the PI controller, which authenticates the time domain simulations numerically as shown by data taps below.

2) IMPACT OF WIND SPEED

Another reason for sub-synchronous oscillation caused by SSR in series compensated DFIG-based system is the wind speed. The system's compensation level of 40% at 2.5 sec is kept constant, while the wind speed is varied to investigate the response of the proposed scheme at changing wind speed. The dynamical responses of output power in p.u at varying wind speeds, i.e., 8 m/s, 10m/s and 12m/s, are studied at the time domain and frequency domain as well to verify the magnitude of oscillations as shown by figure 5 and figure 6. The time domain response with the PI controller at low wind speeds, i.e., 8ms and 10m/s, gives unstable behavior which tends toward stability as wind speed increases, i.e., at 12m/s, shows stable long lasting oscillations as shown in Fig.5(a, b, c). However, these severe unstable amplitude SSO at 8m/s are restricted to critically stable SSO with proposed controller as depicted by Fig.5(a). As the wind speed increases above critical speed, i.e., 8m/s for proposed scheme, the system shows stable and fast settling with time depicted by Figure 5(b, c).

Similarly, through another verification technique, i.e., frequency scanning, the magnitude of SSO is calculated to authenticate the time domain results precisely given by Fig. 6(a, b, c). The magnitude of SSO at power in per-unit (p.u) with under rated wind speed (8m/s) by implementing proposed schemes shows oscillations of 0.0728 p.u, but the conventional PI controller results in dangerously high magnitude of amount 0.289 p.u, depicted by Fig.6(a). As the wind speed increases, the overall decrease in magnitude of SSO can be seen as in Fig.6(b, c) which is 0.198 p.u with the PI controller while it is minimized to 0.038p.u at the wind speed of 12m/s.

B. TOTAL HARMONIC DISTORTIONS (THD) ANALYSIS

Various types of electronic based FACTS devices such as STATCOM and TCSC are proposed to mitigate SSO in series compensated transmission lines. These devices are

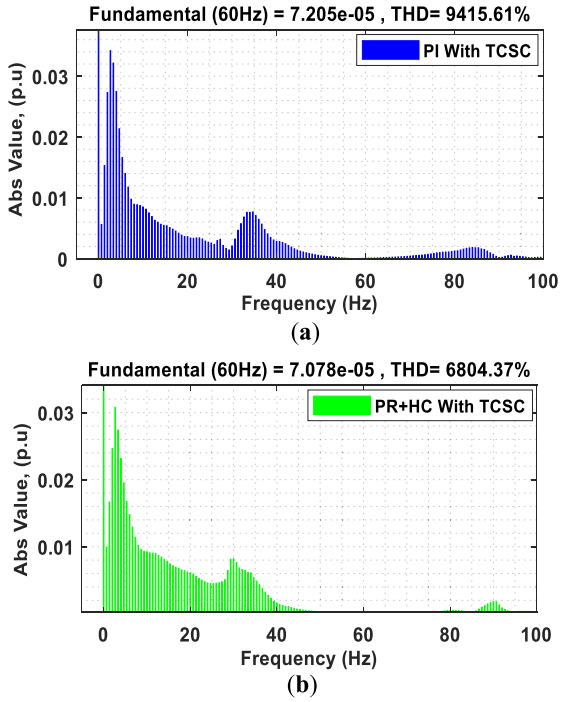

FIGURE 8. THD analysis with the conventional PI controller (a) and the Proposed PR+HC (b) at 30% compensation levels in coordination with TCSC.

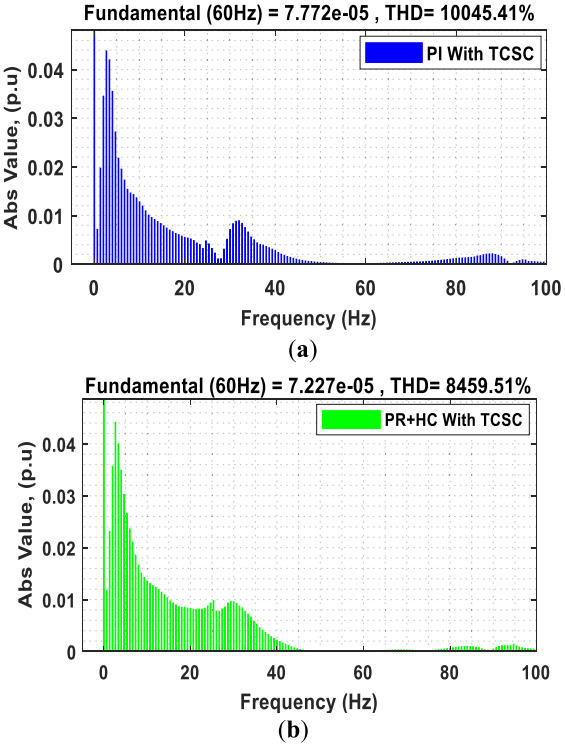

FIGURE 9. THD analysis with the conventional PI controller (a) and the Proposed PR+HC (b) at 40% compensation levels in coordination with TCSC.

comprised of electronic switches to control the impedance of transmission according to the level of compensation. Although FACTS devices can mitigate SSO effectively but

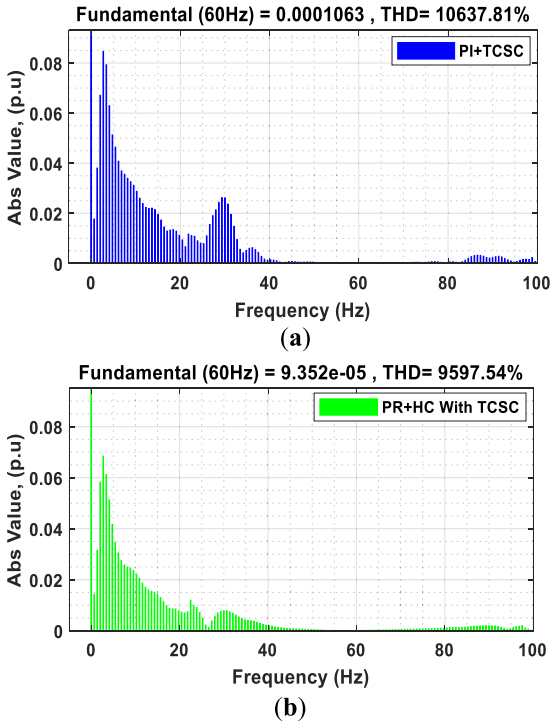

FIGURE 10. THD analysis with the conventional PI controller (a) and the Proposed PR+HC (b) at 50% compensation levels in coordination with TCSC.

can cause harmonic distortions in output power [16], [18]. The harmonic compensator (HC) is additionally included as shown in Fig.2 at the fundamental PR controller to aim enhanced power quality. The time domain response of the proposed control scheme in coordination with TCSC is carried out for two different compensation levels before THD analysis as depicted by Fig.7. In coordination with FACTS devices, it is shown that the designed control scheme, PR+HC, provides comparatively damped and low transient spikes when compared with the PI controller.

To authenticate the non-prominent domain response of power in terms of harmonic analysis, total harmonic distortions (THD) are calculated through fast-Fourier transformation (FFT) analysis. The THD is investigated for three various compensation levels while keeping the wind speed constant at 11m/s. Considering compensation level of 30% as shown by Fig.9, the THD for the PI controller with TCSC is 9415.6% with the magnitude of 7.205e-5, while for the proposed scheme the THD is 6804.3% with 7.07e-5 magnitude. Further, for the 40% of compensation, the THD due to TCSC with the PI controller and the proposed scheme are 10045.4% and 8459.5%, respectively as depicted by Fig.10. Similarly, for the compensation level of 50%, the THD and magnitude of harmonic with proposed scheme, i.e., 10637.8%, are lower than as with the PI controller, i.e., 9597.5% as shown by Fig.10. The overall FFT analysis authenticates that the proposed control scheme results in low magnitude and minimum distortion in the power signal under SSR condition of various compensations.

V. CONCLUSION

This paper focuses on mitigating the SSR problem without compromising on harmonic distortions at DFIG-based wind plant connected to the series-compensated IEEE first benchmark model. The control-based scheme is designed by combination of a PR controller to dampen SSO and HC to minimize the harmonic distortions. The proposed scheme is effectively implemented for damping the SSR issue and compared with the conventionally used PI controller separately and in coordination with TCSC to validate the performance of HC. The time domain and frequency domain simulations authenticate the dampened and fast-settling response of the proposed scheme. Additionally, the low THD response validates the harmonic minimization capability of the designed scheme in cooperative operation with TCSC compared to the PI controller.

In the near future, the converter controlled FACTS devices like STATCOM will be digitalized to mitigate SSR problem in DFIG based wind plant. Furthermore, the Lyapunov function based control of FACTS devices will be designed for robust and stable response at the event of SSR in power system.

APPENDIX

TABLE 1. Test case rated parameters.

Parameters	Values
DC-link Voltage (Vdc)	1150 kV
Rated output power	100 MW
DC-link capacitance	0.67 F
Rated output voltage	575 V
Operating frequency	50Hz
Stator resistance (Rs)	0.023 ohm
Rotor resistance (Rr)	0.016 ohm
Mutual reactance (X_M)	2.9 ohm
Leakage reactance of stator (X_{ls})	0.18
Leakage reactance of rotor (X_{lr})	0.16 ohm
Cut-off frequency (ω_c)	3.2 rad/sec
Transformation ratio	575 V/ 161 kV
Transformer reactance (X_T)	0.14 ohm
Resistance of line (R_l)	0.02 ohm
Reactance of line (X_l)	0.5 ohm

TABLE 2. Control scheme parameters.

Scheme	Parameters	Values
PI	k_p	8
	k_i	40
PR	k_p	0.9
	k_i	5
HC	k_{i3}	80
	k_{i5}	60
	k_{i7}	40

REFERENCES

[1] F. Blaabjerg, Y. Yang, D. Yang, and X. Wang, "Distributed power-generation systems and protection," *Proc. IEEE*, vol. 105, no. 7, pp. 1311–1331, Jul. 2017.
[2] M. M. Haque and P. Wolfs, "A review of high PV penetrations in LV distribution networks: Present status, impacts and mitigation measures," *Renew. Sustain. Energy Rev.*, vol. 62, pp. 1195–1208, Sep. 2016.
[3] S. Tohidi, P. Tavner, R. Mcmahon, H. Oraee, M. R. Zolghadri, S. Shao, and E. Abdi, "Low voltage ride-through of DFIG and brushless DFIG: Similarities and differences," *Electr. Power Syst. Res.*, vol. 110, pp. 64–72, May 2014.
[4] H. Huang and C. Chung, "Adaptive neuro-fuzzy controller for static VAR compensator to damp out wind energy conversion system oscillation," *IET Gener., Transmiss. Distrib.*, vol. 7, no. 2, pp. 200–207, Feb. 2013.
[5] T. Ackermann, *Wind Power in Power Systems*. Hoboken, NJ, USA: Wiley, 2005.
[6] R. Grünbaum, P. Halvarsson, and P. Jones, "Series compensation for extended utilization of power transmission systems," in *Proc. 9th IET Int. Conf. AC DC Power Transmiss. (ACDC)*, Oct. 2010, pp. 1–5.
[7] P. Kundur, *Power System Stability and Control*. New York, NY, USA: McGraw-Hill, 1994.
[8] K. R. Padiyar, *Analysis of Subsynchronous Resonance in Power Systems*. 1st ed. Boston, MA, USA: Kluwer, 1999.
[9] B. Liu, Z. Li, X. Chen, Y. Huang, and X. Liu, "Recognition and vulnerability analysis of key nodes in power grid based on complex network centrality," *IEEE Trans. Circuits Syst. II, Exp. Briefs*, vol. 65, no. 3, pp. 346–350, Mar. 2018.
[10] P. Pourbeik, R. J. Koessler, D. L. Dickmander, and W. Wong, "Integration of large wind farms into utility grids (Part 2—Performance issues)," in *Proc. IEEE Power Eng. Soc. Gen. Meeting*, Toronto, ON, Canada, Mar. 2003, pp. 1520–1525.
[11] K. Narendra, D. Fedirchuk, R. Midence, N. Zhang, A. Mulawarman, P. Mysore, and V. Sood, "New microprocessor based relay to monitor and protect power systems against sub-harmonics," in *Proc. IEEE Electr. Power Energy Conf.*, Winnipeg, MB, Canada, Oct. 2011, pp. 438–443.
[12] L. Wang, X. Xie, H. Liu, Y. Zhan, J. He, and C. Wang, "Review of emerging SSR/SSO issues and their classifications," *J. Eng.*, vol. 2017, no. 13, pp. 1666–1670, Jan. 2017.
[13] L. Wang, X. Xie, Q. Jiang, H. Liu, Y. Li, and H. Liu, "Investigation of SSR in practical DFIG-based wind farms connected to a series-compensated power system," *IEEE Trans. Power Syst.*, vol. 30, no. 5, pp. 2772–2779, Sep. 2015.
[14] W. Chen, X. Xie, D. Wang, H. Liu, and H. Liu, "Probabilistic stability analysis of subsynchronous resonance for series-compensated DFIG-based wind farms," *IEEE Trans. Sustain. Energy*, vol. 9, no. 1, pp. 400–409, Jan. 2018.
[15] X. Zheng, Z. Xu, and J. Zhang, "A supplementary damping controller of TCSC for mitigating SSR," in *Proc. IEEE Power Energy Soc. Gen. Meeting*, Jul. 2009, pp. 1–5. [Online]. Available: https://ieeexplore.ieee.org/document/5275956
[16] F. D. de Jesus, E. H. Watanabe, L. F. W. de Souza, and J. E. R. Alves, "SSR and power oscillation damping using gate-controlled series capacitors (GCSC)," *IEEE Trans. Power Del.*, vol. 22, no. 3, pp. 1806–1812, Jul. 2007.
[17] K. R. Padiyar and N. Prabhu, "Design and performance evaluation of subsynchronous damping controller with STATCOM," *IEEE Trans. Power Del.*, vol. 21, no. 3, pp. 1398–1405, Jul. 2006.
[18] H. A. Mohammadpour and E. Santi, "Sub-synchronous resonance analysis in DFIG-based wind farms: Mitigation methods—TCSC, GCSC, and DFIG controllers—Part II," in *Proc. IEEE Energy Convers. Congr. Expo. (ECCE)*, Sep. 2014, pp. 1550–1557.
[19] L. Fan and Z. Miao, "Mitigating SSR using DFIG-based wind generation," *IEEE Trans. Sustain. Energy*, vol. 3, no. 3, pp. 349–358, Jul. 2012.
[20] P.-H. Huang, M. S. El Moursi, W. Xiao, and J. L. Kirtley, "Subsynchronous resonance mitigation for series-compensated DFIG-based wind farm by using two-degree-of-freedom control strategy," *IEEE Trans. Power Syst.*, vol. 30, no. 3, pp. 1442–1454, May 2015.
[21] A. E. Leon and J. A. Solsona, "Sub-synchronous interaction damping control for DFIG wind turbines," *IEEE Trans. Power Syst.*, vol. 30, no. 1, pp. 419–428, Jan. 2015.
[22] A. E. Leon, "Integration of DFIG-based wind farms into series-compensated transmission systems," *IEEE Trans. Sustain. Energy*, vol. 7, no. 2, pp. 451–460, Apr. 2016.

[23] M. A. Chowdhury and G. M. Shafiullah, "SSR mitigation of series-compensated DFIG wind farms by a nonlinear damping controller using partial feedback linearization," *IEEE Trans. Power Syst.*, vol. 33, no. 3, pp. 2528–2538, May 2018.
[24] C. Karunanayake, J. Ravishankar, and Z. Y. Dong, "Nonlinear SSR damping controller for DFIG based wind generators interfaced to series compensated transmission systems," *IEEE Trans. Power Syst.*, vol. 35, no. 2, pp. 1156–1165, Mar. 2020.
[25] L. Fan, R. Kavasseri, Z. L. Miao, and C. Zhu, "Modeling of DFIG-based wind farms for SSR analysis," *IEEE Trans. Power Del.*, vol. 25, no. 4, pp. 2073–2082, Oct. 2010.
[26] P. S. E. C. IEEE, "IEEE subsynchronous resonance task force of the dynamic system performance working group power system engineering," *IEEE Trans. Power Appar. Syst.*, vol. PAS-96, no. 5, pp. 1565–1572, Sep. 1977.
[27] Y. Lei, A. Mullane, G. Lightbody, and R. Yacamini, "Modeling of the wind turbine with a doubly fed induction generator for grid integration studies," *IEEE Trans. Energy Convers.*, vol. 21, no. 1, pp. 257–264, Mar. 2006.
[28] F. Mei and B. Pal, "Modal analysis of grid-connected doubly fed induction generators," *IEEE Trans. Energy Convers.*, vol. 22, no. 3, pp. 728–736, Sep. 2007.
[29] L. Fan, C. Zhu, Z. Miao, and M. Hu, "Modal analysis of a DFIG-based wind farm interfaced with a series compensated network," *IEEE Trans. Energy Convers.*, vol. 26, no. 4, pp. 1010–1020, Dec. 2011.
[30] D. Zammit, C. S. Staines, M. Apap, and J. Licari, "Design of PR current control with selective harmonic compensators using MATLAB," *J. Electr. Syst. Inf. Technol.*, vol. 4, no. 3, pp. 347–358, Dec. 2017.
[31] K. Lim and J. Choi, "Output voltage regulation for harmonic compensation under islanded mode of microgrid," *J. Power Electron.*, vol. 17, no. 2, pp. 464–475, Mar. 2017.
[32] K. Lim and J. Choi, "Seamless grid synchronization of a proportional+resonant control-based voltage controller considering non-linear loads under islanded mode," *Energies*, vol. 10, no. 10, p. 1514, Sep. 2017.

SAIF UL ISLAM received the bachelor's degree in electrical power engineering from COMSATS University, Abbottabad, Pakistan, in 2013, and the master's degree in electrical and computer engineering from Pusan National University, Busan, South Korea, in 2020. He is currently pursuing the Ph.D. degree with the Electrical Engineering Department, Kyungpook National University, South Korea. He was an Electrical Instructor with the Government Polytechnic Institute Mansehra, Pakistan, from 2014 to 2018.

SOOBAE KIM received the B.S. degree in electronic and electrical engineering from Kyungpook National University (KNU), Daegu, South Korea, in 2002, the M.S. degree from Seoul National University, Seoul, South Korea, in 2004, and the Ph.D. degree from the University of Illinois at Urbana-Champaign, Urbana, IL, USA, in 2014. He is currently an Associate Professor with the Department of Electrical Engineering, KNU. Prior to KNU, he was a Senior Researcher with Korea Electric Power Corporation, from 2004 to 2016. His research interests include power system dynamics, stability, and control.